

Active vibration control of smart composite structures in hygrothermal environment

P.K. Mahato^{*1} and D.K. Maiti²

¹*Mechanical Engineering and MME, Indian School of Mines, Dhanbad-826004, India*

²*Aerospace Engineering, Indian Institute of Technology, Kharagpur-721302, India*

(Received April 11, 2011, Revised August 9, 2012, Accepted September 24, 2012)

Abstract. The composite materials may be exposed to environmental (thermal or hygral or both) condition during their service life. The effect of environmental condition is usually adverse from the point of view of design of composite structures. In the present research study the effect of hygrothermal condition on the design of laminated composite structures is investigated. The active fiber composite (AFC) which may be utilized as actuator or sensor is considered in the present analysis. The sensor layer is used to sense the level of response of the composite structures. The sensed voltage is fed back to the actuator through the controller. In this study both displacement and velocity feedback controllers are employed to reduce the response of the composite laminate within acceptable limit. The Newmark direct time integration scheme is employed along with modal superposition method to improve the computational efficiency. It is observed from the numerical study that the laminated composite structures become weak in the presence of hygrothermal load. The response of the structure can be brought to the acceptable level once the AFC layer is activated through the feedback loop.

Keywords: AFC; hygrothermal; sensor; actuator; active vibration control; preload

1. Introduction

The composite materials may be exposed to moisture and/or temperature during their operation. When exposed to hygral environment, composites absorb moisture. Heat is conducted into the composite materials when they are exposed to thermal environment. The mechanical properties of these structures are degraded when they are expanded due to heat induction or moisture absorption (Wu and Tauchert 1980, SaiRam and Sinha 1991, Youssef *et al.* 2008, Derrien and Gilormini 2009).

The PZT patches have been used as an actuator or sensor for vibration control of structure till date (Bailey and Hubbard 1985, Baz and Poh 1988, Tzou and Tseng 1990, Ray *et al.* 1994, Lim *et al.* 1999, Peng and Hu 2005, Jin *et al.* 2010, Mirzaee *et al.* 2011). The actuation capabilities of PZT are comparatively less due to low piezoelectric coefficient. High control voltage is required for achieving significant amount of active damping in smart structure if the piezoelectric actuators are directly bonded to the structure.

Bent and co-authors (1995, 1997) develop a very efficient actuator containing piezo-fiber bonded

*Corresponding author, Ph.D., E-mail: p_k_mahato@rediffmail.com

in epoxy matrix. The electric field is developed by Inter-Digitated-Electrode (IDE). The electric field is generated along the fiber direction and elongates the fibers. So, the direct actuation effect is achieved. The direction of the fiber along with electrode can be altered to get the actuation effect in desired direction. A few authors work on AFC with IDE electrode and analyze the actuation properties. These are mainly analytical or experimental works (Tan *et al.* 2002, Zhang and Shen 2007). The numerical analysis is also available on open loop control by Azzouz *et al.* (2001) Arafa and Baz (2000). There exists some studies carried out to assess the behavior on active fiber with laminar electrode (Li *et al.* 2007, Ray 2007, Shridharan and Kim 2009).

There exist a limited number of studies done on the vibration control of composite laminate in hygrothermal environment with PZT actuator (Raja *et al.* 2004). Recently Mahato and Maiti (2010a, 2010b), Maiti and Sinha (2011) have been presented flutter control of composite laminate with AFC actuator in hygrothermal environment.

In the present study, it is aimed to utilize AFC sensor/actuator and to control the undesirable response of laminated composite plate in hygrothermal environment. The AFC mathematical model is developed based on the Finite element (FE) code developed in MATLAB. The Newmark's time integration scheme is used to predict time domain response. The closed-loop system is modeled by the use of a PD (proportional-derivative) feedback controller applied to the actuator. Under these forces, the feedback gains directly affect the close-loop system of equations. The closed loop responses are studied with both velocity and displacement feedbacks. The numerical results are generated for various control gains.

2. Mathematical formulation

A finite element formulation of AFC laminated plate is developed using eight noded isoparametric element. The first order shear deformation theory is used to derive the governing equation of the smart plate under hygrothermal load.

The constitutive equations for the AFC layer are

$$\begin{aligned}\{\sigma\} &= [C]\{\varepsilon\} - [e]\{E\} \\ \{D\} &= [e]^T\{\varepsilon\} + [\kappa]\{E\}\end{aligned}\quad (1)$$

The details of the above matrix and vector are given in Mahato and Maiti (2010a).

Considering that the electric field is applied along the fiber direction, the electric field can be expressed as

$$\{E\} = [E_1 \ E_2 \ E_3]^T = [-1/h_{et} \ 0 \ 0]^T V \quad (2)$$

where V is the electric potential difference between two electrode and h_{et} is the electrode spacing of the interdigitated electrode.

If we assume that piezofiber are also at an angle θ_p with x -axis, than the $[e]$ and $[\kappa]$ is transformed into $[e]_{xy}$ and $[\kappa]_{xy}$ respectively and can be written as

$$[e]_{xy} = [T]^{-1}[e][T'], \quad [\kappa]_{xy} = [T']^{-1}[\kappa][T'] \quad (3)$$

$$\text{where, } [T] = \begin{bmatrix} m^2 & n^2 & 2mn \\ n^2 & m^2 & -mn \\ -mn & mn & m^2 - n^2 \end{bmatrix}, \quad [T'] = \begin{bmatrix} m & -n & 0 \\ -n & m & 0 \\ 0 & 0 & 0 \end{bmatrix}; \quad m = \cos\theta_p, \quad n = \sin\theta_p$$

Applying Hamilton's variational principle and substituting and minimizing the total potential energy (including mechanical, electrical potential, piezoelectric external load and mechanical external load) and kinetic energy with respect to global variables leads to three sets of equilibrium equations (Mahato and Maiti 2010a) for substrate layer, actuator layer and sensor layer, respectively, and are given below

$$\begin{aligned} [M]\{\ddot{X}\} + [K_{dd}]\{X\} - [K_{da}]\{V_a\} - [K_{ds}]\{V_s\} &= \{F_1\} \\ [K_{ad}]\{X\} + [K_{aa}]\{V_a\} &= \{F_2\} \\ [K_{sd}]\{X\} + [K_{ss}]\{V_s\} &= 0 \end{aligned} \quad (4)$$

The details of the above matrices and vectors are available in Mahato and Maiti (2010a). The electrical potential of sensor and the derivative with respect to time recovered from

$$\begin{aligned} \{V_s\} &= -[K_{ss}]^{-1}[K_{sd}]\{X\} \\ \{\dot{V}_s\} &= -[K_{ss}]^{-1}[K_{sd}]\{\dot{X}\} \end{aligned} \quad (5)$$

Eliminating $\{V_a\}$ and $\{V_s\}$, the Eq. (4) can be rewritten as

$$[M]\{\ddot{X}\} + [K^*]\{X\} = \{F_1\} + \{F_c\} \quad (6)$$

where $[K^*] = [K_{dd}] + [K_{da}][K_{aa}]^{-1}[K_{ad}] + [K_{ds}][K_{ss}]^{-1}[K_{sd}]$ and $\{F_c\} = [K_{da}][K_{aa}]^{-1}\{F_2\}$ is the control feedback force.

2.1 Control mechanism and modal analysis

A linear PD controller is used. The actuator voltage is expressed as follows

$$\{V_a\} = G_d\{V_s\} + G_v\{\dot{V}_s\} \quad (7)$$

The effect of the piezoelectric sensing voltage on actuation is negligible compared to direct feedback voltage.

The dynamic equation is reduced to modal form. The details of control mechanism and modal formulations are given in Mahato and Maiti 2010b.

2.2 Newmark's time integration scheme and DFT analysis theory

Newmark's direct integration (Bathe 1996) scheme is employed to approximate the time derivatives and thereby to solve the forced vibration equations. The Discrete Fourier Transform (DFT) is used to find out the frequency response from the time history based on Fast Fourier Transform (FFT) algorithm (Mario and Paz 2005).

2.3 Hygrothermal load vector formulations and geometric stiffness

The hygrothermal strains of a lamina which are expressed as

$$\begin{bmatrix} e_x \\ e_y \\ e_{xy} \end{bmatrix}_k = \begin{bmatrix} \beta_x \\ \beta_y \\ \beta_{xy} \end{bmatrix}_k \Delta\chi + \begin{bmatrix} \alpha_x \\ \alpha_y \\ \alpha_{xy} \end{bmatrix} \Delta T \quad (8)$$

β_x , β_y and β_{xy} are the moisture expansion coefficient of a lamina obtained by transformation from β_1 and β_2 . α_x , α_y and α_{xy} are the thermal expansions coefficients obtained in the same manner from α_1 and α_2 . The hygrothermal load vector is formulated from the hygrothermal strain (Mahato and Maiti 2010b).

The hygrothermal loads are considered as initial preload acting on the laminate when the laminate is exposed to hygrothermal environment. The initial preload can be taken care in the dynamic response analysis through geometric stiffness. The geometric stiffness is calculated considering the simplest nonlinear strain displacement relationship as given in details in our previous work (Mahato and Maiti 2010b).

3. Results and discussion

The numerical results obtained based on the developed formulation are presented in the subsequent sections. The developed FE analysis procedure is coded in MATLAB. The codes are established for static and dynamic analysis of smart laminated structure in hygrothermal environment (Mahato and Maiti 2010a, b). The numerical results are generated in the present section using the material properties of graphite/epoxy (Tables 1 and 2) and AFC (Table 3). A square

Table 1 Elastic moduli of graphite/epoxy lamina at different moisture levels (Mahato and Maiti 2010b)

| Elastic Moduli (GPa) | Temperature, T (K) | | | | | |
|-------------------------|----------------------|-------|------|-------|-------|-------|
| | 300 | 325 | 350 | 375 | 400 | 425 |
| E_{11} | 128 | 128.1 | 129 | 130.6 | 131.8 | 131.1 |
| E_{22} | 9.4 | 8.69 | 7.84 | 7.12 | 6.71 | 6.61 |
| G_{12} | 6.28 | 5.88 | 5.33 | 5.07 | 4.66 | 4.6 |

$$G_{13} = G_{12}, G_{23} = 0.5G_{12}, \nu_{12} = 0.3, \alpha_{11} = -0.3310^{-6}/\text{K} \text{ and } \alpha_{22} = 28.1310^{-6}/\text{K}, \rho = 1600 \text{ kg/m}^3$$

Table 2 Elastic moduli of graphite/epoxy lamina at different moisture levels (Mahato and Maiti 2010b)

| Elastic Moduli (GPa) | Moisture Concentration, C (%) | | | | | |
|-------------------------|---------------------------------|------|------|------|------|------|
| | 0.0 | 0.25 | 0.5 | 0.75 | 1.0 | 1.25 |
| E_{11} | 128 | 128 | 128 | 128 | 128 | 128 |
| E_{22} | 9.4 | 7.26 | 6.12 | 5.56 | 5.43 | 5.43 |
| G_{12} | 6.28 | 5.39 | 5.0 | 4.0 | 3.65 | 3.5 |

$$G_{13} = G_{12}, G_{23} = 0.5G_{12}, \nu_{12} = 0.3, \beta_{11} = -0.0 \text{ and } \beta_{22} = 0.44, \rho = 1600 \text{ kg/m}^3$$

Table 3 Estimated properties of AFC - 50% fiber volume fraction (Mahato and Maiti 2010b)

| C_{11} (GPa) | C_{22} (GPa) | C_{12} (GPa) | C_{44} (GPa) | C_{55} (GPa) | C_{66} (GPa) | e_{11} C/m ² | e_{21} C/m ² | e_{24} C/m ² | κ_{11} F/m | κ_{33} F/m |
|-------------------|-------------------|-------------------|-------------------|-------------------|-------------------|------------------------------|------------------------------|------------------------------|------------------------|------------------------|
| 138.1 | 148.9 | 71.15 | 32.35 | 32.35 | 39.14 | 14.14 | -3.34 | 10.79 | 8.599×10^{-9} | 6.485×10^{-9} |

$$\nu_{12} = 0.35, \nu_{13} = 0.38 = \nu_{23}, \rho = 6700 \text{ kg/m}^3$$

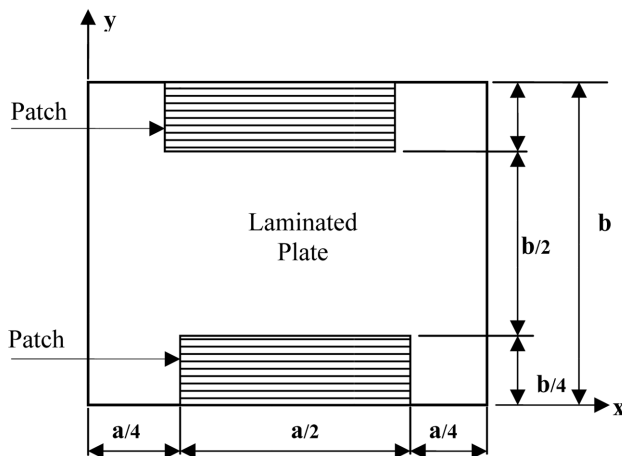


Fig. 1 Simply supported plate model with AFC actuator

($0.6 \times 0.6 \times 0.006$ m) simply supported plate with cross-ply (90/0/90/0) laminate is taken up for the analysis. Only the unsymmetrical laminates are taken except otherwise mention in the present analysis. Because from the previous studies (Mahato and Maiti 2010a, b) it was observed that the hygrothermal effect was more on the unsymmetrical laminates than symmetrical laminates. The mesh density of 8×8 is used throughout the analysis.

The location of AFC patches has been selected based on optimal placement of ACLD treatment as reported in Ro and Baz (2002) which is shown in Fig. 1. Unless otherwise mentioned, the thickness of AFC layer and piezoelectric fiber orientation are considered as 1 mm and 0° , respectively. The boundary conditions are considered as simply-supported at all edges. The effectiveness of the velocity and displacement feedback control strategy for vibration control of the plate is studied here.

3.1 The effect of fiber orientation of AFC

The effect of the variation of (θ_p) of AFC is analyzed using a particular value of velocity feedback gain $G_v = 0.05$. It is assumed that inter-digitated-electrodes (IDE) are always perpendicular to the piezofiber. The values of the fiber orientation angle are taken as $0^\circ, 45^\circ, 60^\circ$ and 90° . Fig. 2 demonstrates the responses of the plate for different θ_p values. It is observed that the maximum performance of the patches is observed when θ_p is 0° . Therefore, the value of θ_p is taken as 0° only for the subsequent analyses.

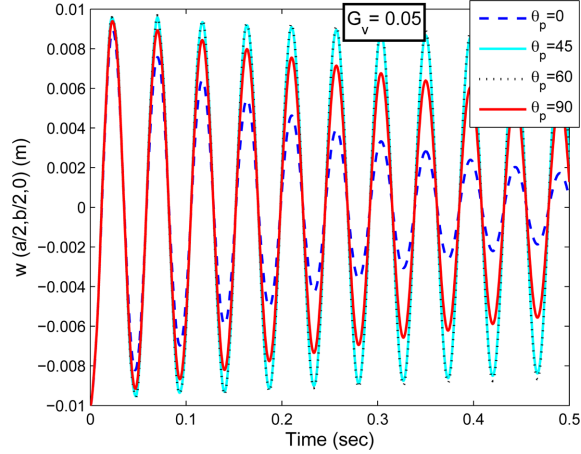


Fig. 2 Effect of fiber orientation (θ_p) of AFC on active control

3.2 Vibration control of laminated plate with initial displacement

In this example, vibration control due to the initial displacement of the simply supported plate is studied. The plate is subjected to a point load of magnitude 1000 N at the center of the laminated plate (90/0/90/0). After having static initial displacement due to the application of point load, the load is suddenly removed and the plate is set into vibration with static deflection as initial displacement and at the same time the feedback control system is activated. The voltage output of the sensor (coupled with a charge amplifier) is amplified and feedback is given to the actuator.

The effect of velocity feedback gain (G_v) is shown in Figs. 3 and 4. The time response of center deflection of the laminated plate is shown in Fig. 3 for different velocity feedback gains. Fig. 4 illustrates the frequency response of the plate. The Fast Fourier Transform (FFT) is used to find out

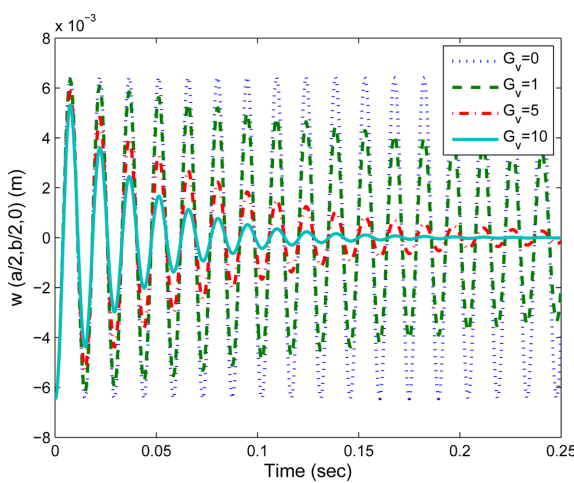


Fig. 3 Time response for different velocity feedback gain

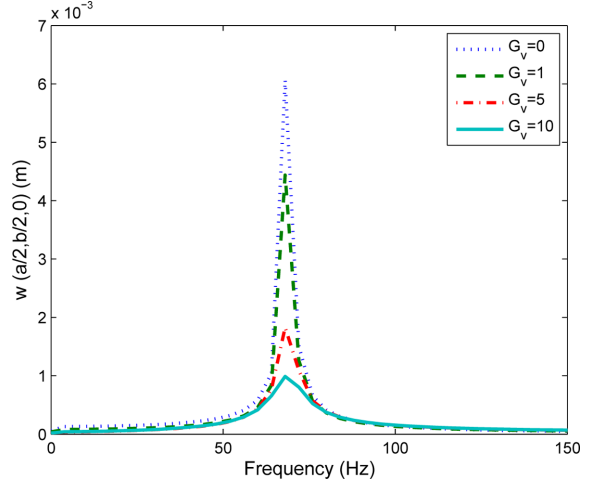


Fig. 4 Frequency response for different velocity feedback gain

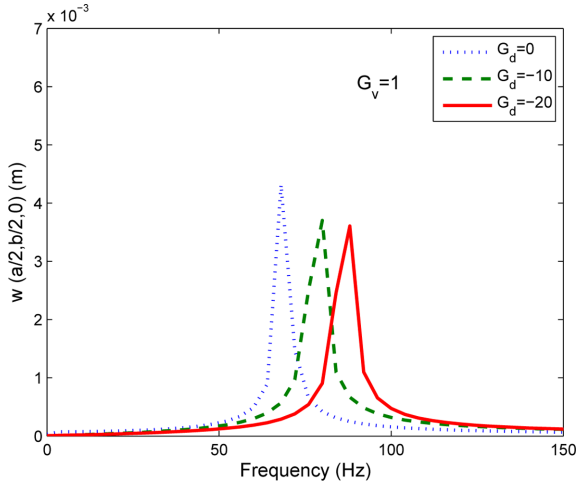


Fig. 5 Frequency response for different displacement feedback gain

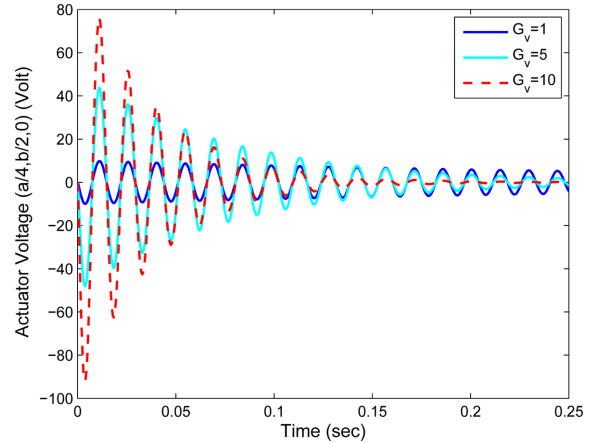


Fig. 6 Control actuator voltage at $x = a/2, y = a/4$

the frequency response from the time history. The values of G_v are varied from 0 to 10. It is to be noted here that the response is unchanged throughout the time history when AFC patch is not activated i.e., $G_v = 0$. The response gradually reduces with time when feedback gain is applied to the actuator. When G_v is increased the response comes to static state quickly because the damping induced by feedback control system increases. The damping in a dynamic system is a dissipative mechanism by which dynamic response is reduced. The damping which dissipates energy in a dynamic system is proportional to velocity. Thus the velocity feedback gain induces active damping in a dynamic system. The values of damping factor are 0.014($\approx 0\%$), 1.30%, 3.59% and 6.52% for $G_v = 0$, $G_v = 1$, $G_v = 5$ and $G_v = 10$ respectively. The damping factors are calculated from frequency response curve employing half power point method at the peak amplitude. The dynamic response can be also controlled by displacement feedback gain (G_d) as shown in Fig. 5. It is observed from the figure that the frequency is higher with the increase in the displacement feedback. This shows that the displacement feedback increases the effective structural stiffness actively.

It is to be stated here that the level of control voltage which is to be fed back to the actuator should be known for smooth and safe performance. Fig. 6 illustrates the time response of the voltage applied to the actuator. It is observed that the control voltages corresponding to the gain are quite nominal. It is assumed that the system is stable at that control voltages.

3.3 Vibration control of laminate in hygrothermal environment with initial displacement

The present analysis is based on the assumption that the moisture and/or temperature content in composite laminate reached the steady state level. The analysis is carried out in thermal environment at first. In the present study, the piezoelectric properties are assumed to be constant in the elevated thermal environment. The frequency response of transverse displacement of the plate is presented in Fig. 7 for various elevated temperatures and with velocity feedback. It is observed from Fig. 7 that the fundamental frequency is reduced gradually with increase in temperature and the corresponding amplitudes are increased. The 1st mode frequency of the plate at $\Delta T = 0$, $\Delta T = 10$

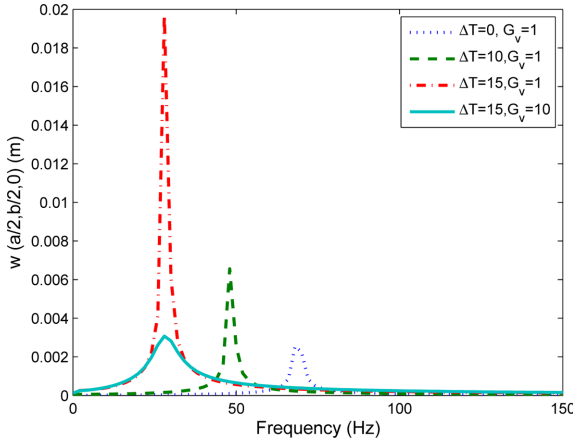


Fig. 7 Frequency response (w) of plate ($a/2, b/2, 0$) due to initial displacement in thermal environment

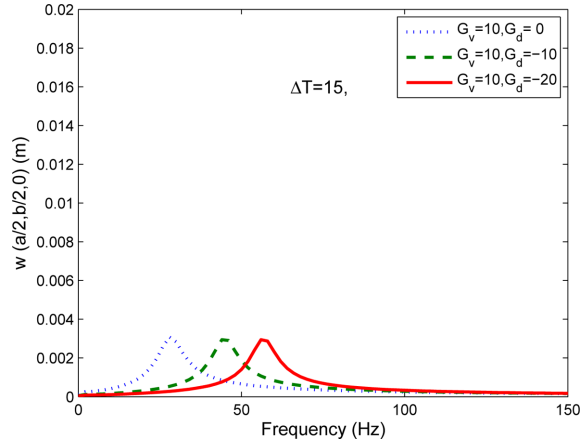


Fig. 8 Frequency response (w) of plate ($a/2, b/2, 0$) due to initial displacement in thermal environment with different displacement feedback gain

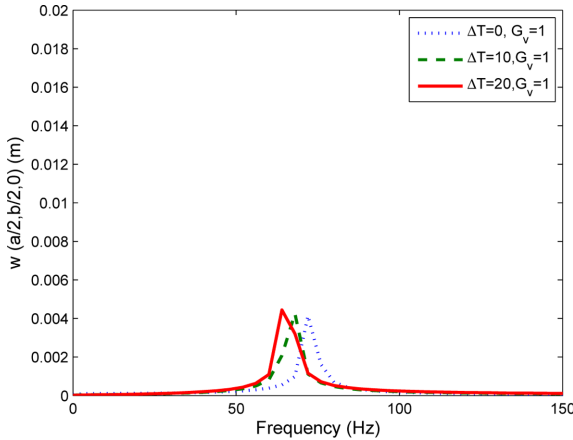


Fig. 9 Frequency response (w) of symmetric (0/90/90/0) plate ($a/2, b/2, 0$) due to initial displacement in thermal environment

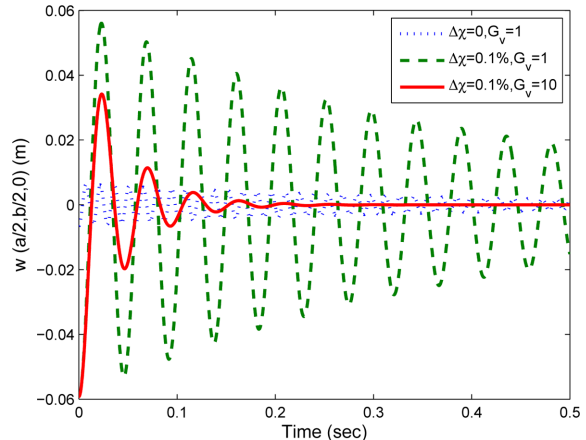


Fig. 10 Time response of plate due to initial displacement in hygral environment

and $\Delta T = 15$ are 68.1 Hz, 48.3 Hz and 28.0 Hz respectively. The amplitude of vibration can be reduced by increasing velocity feedback gain ($G_v = 10$) which induces active damping in the system. The damping factor is calculated and it is found that it increases from 2.84% to 13.36% when G_v is increased from 1 to 10. The fundamental frequency can be enhanced when the displacement feedback (G_d) is activated along with G_v (Fig. 8). The numerical experimentation has also been carried out for a symmetric laminate (0/90/90/0) to show the thermal effect. The thermal effect for the above laminate is shown in the Fig. 9. It is observed from the analysis that the effect is very less for a symmetric laminate.

Now it is considered that the plate is exposed to hygral environment. The time responses and frequency responses of the plate are shown in Figs. 10 and 11 respectively in hygral environment

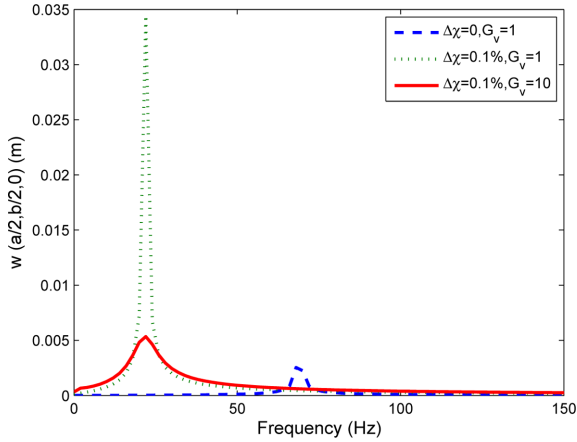


Fig. 11 Frequency response of plate due to initial displacement in hygral environment

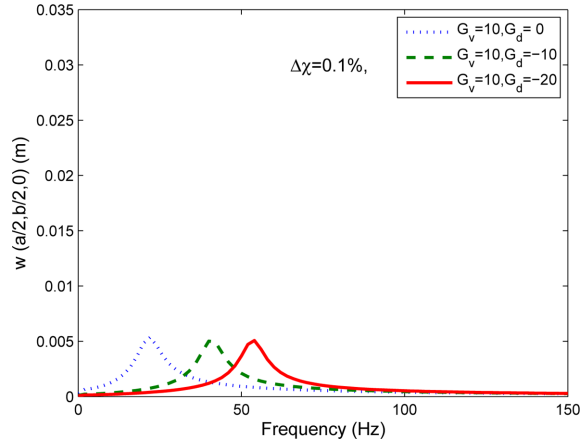


Fig. 12 Frequency response of plate due to initial displacement in hygral environment with different displacement feedback gain

($\Delta\chi = 0.1\%$). It is observed from these figures that the response is increased with increase in moisture concentration. The frequency is also reduced. The response is controlled by increasing the $G_v = 10$ in the similar line of thermal effect and the active damping is calculated as 16.24%. The frequency can also be enhanced by applying displacement feedback gain (G_d) with G_v as shown in Fig. 12. It is also observed that the stiffness is increased when the G_d is increased although the damping is reduced slightly.

3.4 Vibration control of laminate in hygrothermal environment due to time-harmonic force

A distributed pressure load of intensity $q_0 = 1000$ N is considered on the top of the plate which is varying sinusoidally at the frequency of 50 Hz. The time dependent dynamic pressure is applied for the duration of 100 ms only. Fig. 13 illustrate the time response at center ($a/2, b/2, 0$) of the plate in

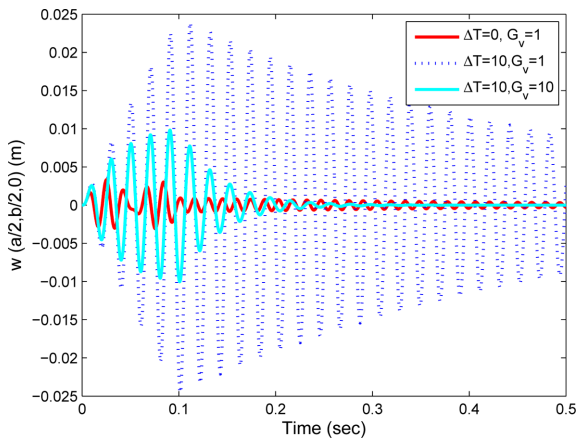


Fig. 13 Time response of plate due to distributed load varying sinusoidally (thermal)

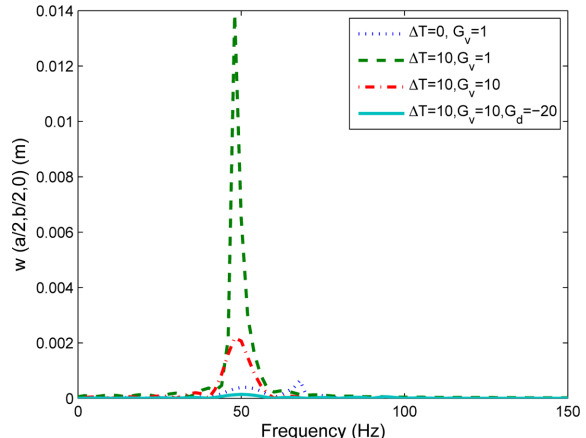


Fig. 14 Frequency response of plate due to distributed load varying sinusoidally

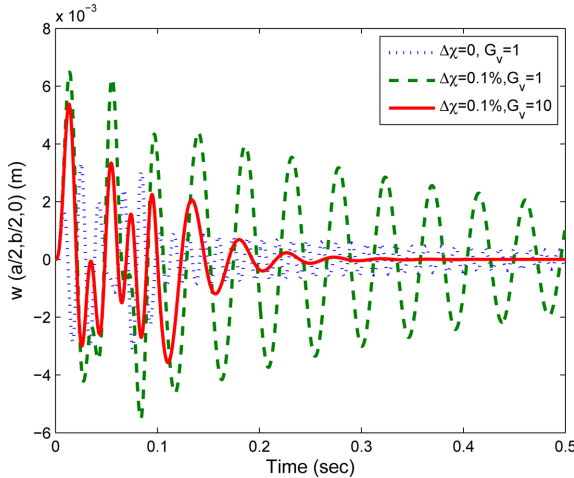


Fig. 15 Time response of plate due to distributed load varying sinusoidally (hygral)

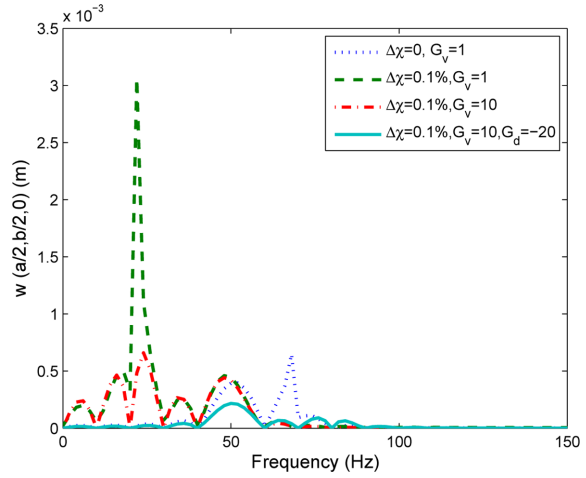


Fig. 16 Frequency response of plate due to distributed load varying sinusoidally

thermal environment. It is observed that the response is increased when the plate is exposed to thermal environment ($\Delta T = 10$). The response can be reduced by increasing the gain from $G_v = 1$ to $G_v = 10$. The frequency response of the plate is shown in Fig. 14 for the sinusoidal loading. The damping values are calculated for the dominating peak of the frequency response curve. It is observed that the damping values increases from 1.87% to 6.0% when the values of G_v are increased from 1 to 10. The damping factor increases upto 8.83% displacement feedback is activated with $G_d = -20$ along with G_v .

Figs. 15, 16 illustrate the time response and frequency response of the plate in hygral environment. The response is increased when the plate is exposed to moisture concentration of 0.1% ($\Delta\chi = 0.1\%$). It is controlled by increasing velocity feedback gain $G_v = 10$ from $G_v = 1$ because the damping increases to 9.2% from 3.5%. From the frequency response plot it is observed that the dominating frequency is sifted to higher value i.e. the stiffness is increased when displacement feedback ($G_d = -20$) is activated along with velocity feedback ($G_v = 10$). It is also to be noted here that the sinusoidal load induces more number of modes to be participated in the dynamic response unlike previous study. It is obvious because the forcing frequency (50 Hz) is higher than the first natural frequency (21.8 Hz) in that environment.

4. Conclusions

The FE program is developed in MATLAB environment to study the effect of hygrothermal load on the analysis and design of laminated composite structures. The FE program can also take care of modeling of AFC sensor and actuator and feedback loop. It is observed that the response of laminated composite structures is increased in the hygrothermal environment. This is due to the reduction of effective stiffness of the laminate. The effective stiffness of the laminate reduces because of induction of compressive initial stress in hygrothermal environment. This can be corroborated from the observation of the frequency response plot. The response can be brought to

acceptable limit once the close loop control technique is activated. It is observed from numerical study that the velocity feedback loop offers a sufficiently high effective damping to reduce the response of the laminated composite structures in hygrothermal environment. The stiffness can also be enhanced by applying displacement feedback. The overall performance of a laminate can be enhanced when both velocity and displacement feedback are activated.

References

- Arafa, M. and Baz, A. (2000), "Dynamic of active piezoelectric damping composites", *Compos. Part B*, **31**, 255-264.
- Azzouz, M.S., Mei, C., Bevan, J.S. and Ro, J.J. (2001), "Finite element modeling of MFC/AFC actuators and performance of MFC", *J. Intell. Mater. Syst. Struct.*, **12**, 601-612.
- Bailey, T. and Hubbard, J.E. Jr. (1985), "Distributed piezoelectric-polymer active vibration control of a cantilever beam", *J. Guid Control Dyn.*, **8**(5), 605-611.
- Bathe, K.J. (1995), *Finite Element Procedures*, 2nd Edition, Prentice Hall.
- Baz, A. and Poh, S. (1988), "Performance of an active control system with piezoelectric actuators", *J. Sound Vib.*, **126**, 327-343.
- Bent, A.A., Hagood, N.W. and Rodgers, J.P. (1995), "Anisotropic actuation with piezoelectric fiber composites", *J. Intell. Mater. Syst. Struct.*, **6**, 338-349.
- Bent, A.A. (1997), "Active fiber composites for structural actuation", PhD Thesis, MIT.
- Derrien, K. and Gilormini, P. (2009), "The effect of moisture-induced swelling on the absorption capacity of transversely isotropic elastic polymer-matrix composites", *Int. J. Solid Struct.*, **46**, 1547-1553.
- Jin, Z.L., Yang, Y.W. and Soh, C.K. (2010), "Semi-analytical solutions for optimal distributions of sensors and actuators in smart structure vibration control", *Smart Struct. Syst.*, **6**(7), 767-792.
- Li, Q., Mei, C. and Huang, J.K. (2007), "Suppression of thermal postbuckling and nonlinear panel flutter motions using piezoelectric actuators", *AIAA J.*, **45**(8), 1861-1873.
- Lim, Y.H., Varadan, V.V. and Varadan, V.K. (1999), "Closed loop finite-element modeling of active structural damping in the time domain", *Smart Mater. Struct.*, **8**, 390-400.
- Mahato, P.K. and Maiti, D.K. (2010a), "Flutter control of smart composite structure in hygro-thermal environment", *J. Aerosp. Eng.*, **23**(4), 317-326.
- Mahato, P.K. and Maiti, D.K. (2010b), "Aeroelastic analysis of smart composite structures in hygrothermal environment", *Compos. Struct.*, **92**(4), 1027-1038.
- Maiti, D.K. and Sinha, P.K. (2011), "Analysis of smart laminated composites employing piezo embedded super element", *Proc. Eng.*, **14**, 3268-2376.
- Mirzaee, E., Eghtesad, M. and Fazelzadeh, S.A. (2011), "Trajectory tracking and active vibration suppression of a smart single-link flexible arm using a composite control", *Smart Struct. Syst.*, **7**(2), 103-116.
- Paz, M. (2003), *Structural Dynamics : Theory and Computation*, 4th Edition, KPuwer Academic Publishers.
- Peng, F., Ng, A. and Hu, Y.R. (2005), "Actuator placement optimization and adaptive vibration control of plate smart structure", *J. Intell. Mater. Syst. Struct.*, **16**, 263-271.
- Raja, S., Sinha, P.K., Prathap, G. and Dwarakanathan, D. (2004), "Influence of active stiffening on dynamic behaviour of piezo-hygro-thermo-elastic composite plates and shells", *J. Sound Vib.*, **278**, 257-283.
- Ray, M.C., Bhattacharya, R. and Samanta, B. (1994), "Static analysis of an intelligent structure by the finite element method", *Comput. Struct.*, **52**(4), 617-631.
- Ray, M.C. (2007), "Smart damping of laminated thin cylindrical panels using piezoelectric fiber reinforced composites", *I. J. Solid Struct.*, **44**, 587-602.
- Ro, J. and Baz, A. (2002), "Optimum placement and control of active constrained layer damping using modal strain energy approach", *J. Vib. Control*, **8**, 861-876.
- SaiRam, K.S. and Sinha, P.K. (1991), "Hygrothermal effects on the bending characteristics of laminated composite plates", *Comput. Struct.*, **40**(4), 1009-1015.
- Shridharan, S. and Kim, S. (2009), "Piezo-electric control of stiffened panels subject to interactive buckling", *Int.*

- J. Solid Struct.*, **46**, 1527-1538.
- Tan, P., Tong, L. and Sun, D. (2002), "Dynamic characteristics of a beam system with active piezoelectric fiber reinforced composite layers", *Compos. Part B*, **33**, 545-555.
- Tzou, H.S. and Tseng, C.I. (1990), "Distributed piezoelectric sensor/actuator design for dynamic measurement/control of distributed parameter systems - a piezoelectric finite element approach", *J. Sound Vib.*, **138**(1), 17-34.
- Wu, C.H. and Tauchert, T.R. (1980), "Thermoelastic analysis of laminated plates. 2: Antisymmetric cross-ply and angle-ply laminates", *J. Therm. Stress.*, **3**, 365-378.
- Youssef, Z., Jacquemin, F., Gloaguen, D. and Guillen, R. (2008), "A multi-scale analysis of composite structures-Application to the design of accelerated hygrothermal cycles", *Compos. Struct.*, **82**, 302-309.
- Zhang, H.Y. and Shen, Y.P. (2007), "Vibration suppression of laminated plates with 1-3 piezoelectric fiber-reinforced composite layers equipped with interdigitated electrodes", *Compos. Struct.*, **79**, 220-228.

Notations

| | |
|----------------------|---|
| a (subscript) | : Actuator |
| T | : Temperature |
| $[e]$ | : Piezoelectric matrix |
| V | : Voltage |
| s (subscript) | : Sensor |
| $\{X\}$ | : The global displacement vector |
| $[C]$ | : Constitutive relation matrix |
| $\{D\}$ | : Electrical displacement vector |
| $[\kappa]$ | : Dielectric matrix |
| $\{E\}$ | : Electric field |
| $\{F_1\}$ | : Mechanical load vector |
| $\{F_2\}$ | : Piezo-electric load vector |
| χ | : Moisture |
| $[K_{aa}], [K_{ss}]$ | : Piezo-electric stiffness |
| G_d | : Displacement feedback gain |
| $[K_{da}], [K_{ds}]$ | : Electro-mechanical coupling stiffness |
| G_v | : Velocity feedback gain |
| $[K_{dd}]$ | : Mechanical stiffness matrix |
| θ_p | : Piezofiber orientation angle |
| $[M]$ | : Mass matrix |
| $[T], [T']$ | : Transformation matrix |